



State Observer with Round-Robin Aperiodic Sampled Measurements with Jitter

Antonino Sferlazza, Luca Zaccarian, Sophie Tarbouriech

► To cite this version:

Antonino Sferlazza, Luca Zaccarian, Sophie Tarbouriech. State Observer with Round-Robin Aperiodic Sampled Measurements with Jitter. *Automatica*, 2021, 129, pp.109573. <10.1016/j.automatica.2021.109573>. <hal-03427393>

HAL Id: hal-03427393

<https://laas.hal.science/hal-03427393v1>

Submitted on 13 Nov 2021

HAL is a multi-disciplinary open access archive for the deposit and dissemination of scientific research documents, whether they are published or not. The documents may come from teaching and research institutions in France or abroad, or from public or private research centers.

L'archive ouverte pluridisciplinaire **HAL**, est destinée au dépôt et à la diffusion de documents scientifiques de niveau recherche, publiés ou non, émanant des établissements d'enseignement et de recherche français ou étrangers, des laboratoires publics ou privés.



HAL Authorization

State Observer with Round-Robin Aperiodic Sampled Measurements with Jitter

Antonino Sferlazza^a, Sophie Tarbouriech^b, Luca Zaccarian^{b,c}

^a*Department of Engineering, University of Palermo, 90128 Palermo, Italy*

^b*LAAS-CNRS, Université de Toulouse, CNRS, F-31400 Toulouse, France*

^c*Dipartimento di Ingegneria Industriale, University of Trento, Italy*

Abstract

A sampled-data observer is proposed for linear continuous-time systems whose outputs are sequentially sampled via non-uniform sampling intervals repeating a prescribed Round-Robin sequence. With constant sampling intervals (jitter-free case) we provide constructive necessary and sufficient conditions for the design of an asymptotic continuous-discrete observer whose estimation error is input-to-state stable (ISS) from process disturbances and measurement noise. We use a time-varying gain depending on the elapsed time since the last measurement. With non-constant sampling intervals (jitter-tolerant case), our design conditions are only sufficient. A suspension system example shows the effectiveness of the proposed approach.

Key words: Sampled-data observer, aperiodic measurements, hybrid systems, linear systems, Round-Robin scenario.

1 Introduction

The observation, estimation and control problems for dynamical systems using data transmitted over communication networks attracted several works in the past decade, dealing with lossy and intermittent data, and with network reliability, as surveyed in [23]. In the specific case where the output is only available at isolated time instants, the classical estimation paradigms, using continuous plant measurements from the plant, need to be revisited. (see, e.g., [22,9,25,37,11,10,31] and the references therein).

When the measurements are available periodically, many algorithms are available, based on discrete-time observers for the discretized plant; see, e.g. [28], [5] and references therein. However, often this approach is not realistic because the elapsed time between two measurements is not constant (sporadic measurements). In order to address this problem, [32] and [3], propose a method for nonlinear Lipschitz systems with sampled measurements. For the same class of nonlinear Lipschitz systems, [12] and [13] propose design techniques for the injection gain based on Linear Ma-

trix Inequalities (LMIs) certifying asymptotic stability of the error dynamics. Moreover, in [13] high-gain observers are considered. In [27] and [4], nonlinear uniformly observable single output systems are addressed. Finally, some classes of systems with sampled and delayed outputs are addressed in [26]. This estimation problem has also been addressed in a stochastic framework. For example Extended Kalman Filters (EKF) with sporadic measurements have been proposed in many works [35], [30], [24], [38], [6], [14] and [15], where the Kalman filter is adapted to linear and/or nonlinear continuous-discrete system with multirate sampled outputs.

A natural framework to model the coexistence of continuous-time and discrete-time dynamics is that of hybrid dynamical systems [18]. In particular, [16] and [34] propose hybrid observers for linear systems with sampled measurements where the output error injection gain (constant in [16] and time-varying in [34]) is computed by means of LMI-based conditions embedding the matrix exponential. In both these works, the LMIs proposed are infinite-dimensional and are solved by suitable sequential algorithms, as in [34], or by convex approximations of the exponential matrix, as in [16]. Nonlinear Lipschitz systems have also been cast in the hybrid dynamical systems framework, see e.g. [17] where the problem of exponentially estimating the state is considered.

In this paper we consider linear plants with sampled and sporadic measurements, extending the concepts presented in [34] by assuming that multiple plant outputs are accessible

* Corresponding author A. Sferlazza. Tel. +39 091-23863617. Research supported in part by ANR via grant HANDY, number ANR-18-CE40-0010.

Email addresses: antonino.sferlazza@unipa.it (Antonino Sferlazza), tarbour@laas.fr (Sophie Tarbouriech), zaccarian@laas.fr (Luca Zaccarian).

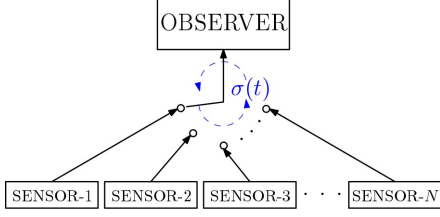


Fig. 1. Round Robin measurement scheme.

following a prescribed and cyclic sequence in a Round-Robin scenario. Such sequential readings are common in many application fields, especially in the presence of sensors networks (see e.g. [25], [1] and references therein) that share the same communication bus, or when the estimation algorithm is implemented in a serial communication hardware platform that only allows for one measurement at a time (see e.g. [2] and references therein, for the case of indoor localization). Our approach largely exploits the sequential nature of the measurement and is somewhat complementary to the recently proposed results of [25], where multiple sensors are collected in sparse order, thereby needing stronger decrease conditions on the arising Lyapunov function. We exploit this advantage by proving that our analysis and design conditions are necessary for the jitter-free case. To this end, we prove a necessary structural collective detectability condition, independent of the observer architecture. In addition to proving exponential estimation, we also prove input-to-state stability (ISS) of our observer with respect to continuous-time process disturbances and impulsive measurement noise.

Notation. \mathbb{N} denotes all positive integers. Given a matrix A , A^T denotes its transpose. Given a full row-rank matrix C , C^\perp denotes its orthogonal complement, namely a matrix such that $[C^\perp \ C^T]$ is square and nonsingular, and such that $CC^\perp = 0$. Given a symmetric matrix S , $\lambda_m(S)$ and $\lambda_M(S)$ denote, respectively, its minimum and maximum (real) eigenvalues, and $S > 0$ (resp. $S < 0$) means that S is positive (resp. negative) definite. The symbol \star denotes a symmetric term.

2 Asynchronous Observations

2.1 Problem data and main estimation goal

In this work we address state estimation problems for the following continuous-time plant,

$$\dot{\bar{x}} = A\bar{x} + Bu + d, \quad (1)$$

where $\bar{x} \in \mathbb{R}^n$ is the unknown state to be estimated, $u : [0, \infty) \rightarrow \mathbb{R}^q$ is a known input and $d : [0, \infty) \rightarrow \mathbb{R}^n$ is an unknown process disturbance, both belonging to the class of locally bounded measurable functions, $A \in \mathbb{R}^{n \times n}$, and $B \in \mathbb{R}^{n \times q}$ are known matrices.

We assume that plant (1) is equipped with $N \in \mathbb{N}$ sensors indexed by integer $\sigma \in \mathcal{S}_N := \{1, 2, \dots, N\}$, providing measurement outputs $y_\sigma \in \mathbb{R}^{m_\sigma}$ (possibly of different dimensions), that are sequentially and asynchronously accessible at non-periodic and strictly increasing discrete instants of time t_k , $k \in \mathbb{N}$ according to a Round-Robin polling mechanism,

as shown in Fig. 1, which well represents the sequential values taken by the sampling function $t_k \mapsto \sigma(t_k) \in \mathcal{S}_N$. More specifically, the Round-Robin mechanism can be written as

$$\sigma(t_{k+1}) = \Gamma(\sigma(t_k)) := \begin{cases} \sigma(t_k) + 1 & \text{if } \sigma(t_k) < N, \\ 1 & \text{if } \sigma(t_k) = N. \end{cases} \quad (2)$$

For example in the case of three sensors, we have $(\sigma(t_1), \sigma(t_2), \sigma(t_3), \sigma(t_4), \sigma(t_5), \dots) = (1, 2, 3, 1, 2, \dots)$.

The sequentially accessible output are a sequence of vectors (possibly of non-uniform dimensions m_σ) written as

$$y_{\sigma(t_k)}(t_k) := C_{\sigma(t_k)}\bar{x}(t_k) + w(k), \quad (3)$$

where w represents a sequence of bounded measurement noise and matrices $C_\sigma \in \mathbb{R}^{m_\sigma \times n}$ satisfy the assumption below. Since input u is accessible, we may easily transform into (3) any output also depending on u via a feed-through term $D_{\sigma(t_k)}u(t_k)$, therefore the strictly proper expression in (3) is non-restrictive.

Assumption 1 Function $t \mapsto u(t)$ is known. Moreover, for each $\sigma \in \mathcal{S}_N$, matrix C_σ is full row rank.

From (2), measurements (3) can be called *asynchronous* because the different outputs y_σ , $\sigma \in \mathcal{S}_N$ are not available at the same time. The Round-Robin structure (2) allows us to model such asynchronous behavior with a single timer, whereas more sophisticated (non-sequential) sampling patterns occurring in network communication often require multiple timers [29]. The aperiodic and sporadic nature of the measurement times t_k , $k \in \mathbb{N}$ is captured by the next assumption.

Assumption 2 For each $\sigma \in \mathcal{S}_N$, there exist scalars T_{m_σ} and T_{M_σ} , with $0 < T_{m_\sigma} \leq T_{M_\sigma}$, such that:

$$T_{m_\sigma(t_k)} \leq |t_{k+1} - t_k| \leq T_{M_\sigma(t_k)} \quad \forall k \in \mathbb{N}. \quad (4)$$

Aperiodicity is captured by the fact that constants T_{m_σ} and T_{M_σ} depend on the sensor σ involved in the measurement. Note also that T_{m_σ} is greater than zero so that two subsequent measurements are never simultaneously available. This feature prevents Zeno behavior in the hybrid model developed in this work.

Definition 1 Consider plant (1) with outputs (3) available at measurement times t_k , $k \in \mathbb{N}$ satisfying Assumptions 1 and 2, we denote by

- Jitter-free scenario: the case where $T_{m_\sigma} = T_{M_\sigma}$, namely the elapsed time between successive measurements y_σ and $y_{\Gamma(\sigma)}$ is constant, for each $\sigma \in \mathcal{S}_N$;
- Jitter-tolerant scenario: the case where $T_{m_\sigma} < T_{M_\sigma}$, namely the elapsed time between y_σ and $y_{\Gamma(\sigma)}$ is not constant for at least one $\sigma \in \mathcal{S}_N$.

Our main contribution is to construct estimators addressing the two scenarios introduced in Definition 1 and ensuring the following asymptotic estimation property.

Goal 1 Given plant (1) with outputs (3) available at measurement times t_k , $k \in \mathbb{N}$ satisfying Assumptions 1 and 2,

build a continuous-discrete observer providing an asymptotic estimate $t \mapsto \hat{\bar{x}}(t)$ of \bar{x} satisfying the following robust uniform exponential bound, for some suitable positive constants M , λ and γ

$$|\bar{x}(t) - \hat{\bar{x}}(t)|^2 \leq M e^{-\lambda t} |\bar{x}(0) - \hat{\bar{x}}(0)|^2 + \gamma \|d\|_{t,\infty}^2 + \gamma \|w\|_{j,\infty}^2, \quad (5)$$

for any initial condition $\bar{x}(0)$ and $\hat{\bar{x}}(0)$ and any exogenous inputs d and w such that:

$$\|d\|_{t,\infty} := \sup_{t \in \mathbb{R}_{\geq 0}} |d(t)| < \infty, \quad \|w\|_{j,\infty} := \sup_{j \in \mathbb{N}} |w(j)| < \infty. \quad (6)$$

Due to the hybrid nature of system (1)–(3) and the ensuing coexistence of continuous-time d and impulsive w disturbances in (5), we cannot follow standard Lyapunov-based optimization techniques for minimizing scalar γ in bound (5). Instead, we only ensure the existence of a finite gain γ in this work, saving as future work optimized designs, possibly using results from [7]. With reference to our main goal we provide, in the next sections,

- *analysis conditions*: establishing whether a specific pre-defined observer ensures Goal 1;
- *design conditions*: leading to the constructive design of an observer ensuring Goal 1.

2.2 Necessary detectability conditions

As a first step in characterizing necessary conditions for state estimation, consider any selection T_σ , $\sigma = \{1, \dots, N\}$ of intersample intervals satisfying

$$T_{m\sigma} \leq T_\sigma \leq T_{M\sigma}, \quad \forall \sigma \in S_N \quad (7)$$

(such a selection is unique if and only if we address the jitter-free case in Def. 1), and note that considering the zero input case, we may gather each sequence of N measurements at the beginning of the corresponding cumulative interval $T := \sum_{\sigma=1}^N T_\sigma$ by defining the output matrix

$$C := \text{col}(C_1 e^{AT_1}, C_2 e^{A(T_1+T_2)}, \dots, C_N e^{AT}). \quad (8)$$

A necessary condition for the solvability of Goal 1 can be stated by considering any possible sequence of intersample intervals T_σ , $\sigma = \{1, \dots, N\}$ and requiring that matrix C in (8) satisfies a suitable discrete-time detectability property.

Proposition 1 *Given plant (1) with outputs (3), Goal 1 can be solved only if for any sequence of intersample intervals T_σ , $\sigma = \{1, \dots, N\}$ satisfying (7), pair (C, e^{AT}) is detectable in the discrete-time sense, where $T := \sum_{\sigma=1}^N T_\sigma$ is the cumulative intersample time and C is the cumulative output matrix in (8).*

Proposition 1 provides insight about the fact that increasing $T_{M\sigma}$ imposes increasingly large sets of detectability conditions. For example, with exponentially unstable selections of A , one expects the necessary conditions of Proposition 1 not to hold for large enough selections of $T_{M\sigma}$.

Proof of Proposition 1. Assume that there exists a sequence of intersample intervals T_σ , $\sigma = \{1, \dots, N\}$ satisfying (7) for which (C, e^{AT}) is not detectable. Then from standard detectability theory, there exists a nonconverging solution of the discrete-time system $z^+ = e^{AT} z$ producing outputs $Cz = 0$ at all (discrete) times. Since $z^+ = e^{AT} z$ is the exact discretization of (1) at the cumulative periodic intervals $\bar{t}_k = kT$, $k \in \mathbb{Z}_{\geq 0}$, then also plant (1) exhibits a nonconverging continuous-time evolution \bar{x} such that the periodically sampled outputs $\bar{y}(\bar{t}_k) = C\bar{x}(\bar{t}_k)$ are all zero. Finally, such an evolution also produces zero outputs from measurements (3), when selecting the measurement times t_k such that $t_{k+1} - t_k = T_{\sigma(t_k)}$ for all $k \in \mathbb{N}$. Indeed, the corresponding outputs can be all computed as

$$\begin{aligned} \begin{bmatrix} y_{\sigma(t_{hN+1})} \\ \vdots \\ y_{\sigma(t_{hN+N})} \end{bmatrix} &= \begin{bmatrix} C_1 \bar{x}(t_{hN+1}) \\ \vdots \\ C_N \bar{x}(t_{hN+N}) \end{bmatrix} = \begin{bmatrix} C_1 e^{AT_1} \bar{x}(t_{hN}) \\ \vdots \\ C_N e^{AT} \bar{x}(t_{hN}) \end{bmatrix} \\ &= C \bar{x}(t_{hN}) = C e^{hAT} \bar{x}(0) = 0. \end{aligned}$$

The proof is completed by noting that the measurement times t_k , $k \in \mathbb{N}$ considered above satisfy (4) because scalars T_σ satisfy (4). As a consequence, Goal 1 cannot be ensured because there is a nonconverging evolution of (1) whose sampled outputs all are zero, thereby being indistinguishable from the zero solution. \square

3 Observer Structure and its properties

3.1 Hybrid model of asynchronous observations

To formalize the set-up described in Section 2.1, we propose a hybrid model using the framework¹ of [18]:

$$\dot{x} = Ax + Bu + d, \quad \dot{\tau} = 1, \quad \dot{\sigma} = 0, \quad (\tau, \sigma) \in C, \quad (9a)$$

$$x^+ = x, \quad \tau^+ = 0, \quad \sigma^+ = \Gamma(\sigma), \quad (\tau, \sigma) \in \mathcal{D}, \quad (9b)$$

$$y_\sigma = C_\sigma x + w, \quad (9c)$$

where $\Gamma(\sigma)$ is defined in (2), and the flow set C and jump set \mathcal{D} are selected as:

$$\begin{aligned} C &:= \bigcup_{\sigma \in S_N} ([0, T_{M\sigma}] \times \{\sigma\}), \\ \mathcal{D} &:= \bigcup_{\sigma \in S_N} ([T_{m\sigma}, T_{M\sigma}] \times \{\sigma\}). \end{aligned} \quad (9d)$$

The extra variable τ in (9a)–(9b) reproduces a timer keeping track of the elapsed time since the last sample.

With model (9), proceeding as in [8, Prop. 1.1] we may show that any sequence of Round-Robin measurements (3) from plant (1) satisfying Assumptions 1 and 2 can be reproduced by output y_σ of (9) evaluated at jump times t_k , $k \in \mathbb{N}$ of a (hybrid) solution to (9), and viceversa. As a consequence,

¹ To simplify the exposition, using a slight abuse of notation we specify the flow and jump sets C and \mathcal{D} as subsets of the domain of states (τ, σ) , without referring to state variable x . This means that the x variable can assume any value in \mathbb{R}^n both in C and \mathcal{D} .

one can equivalently represent the continuous evolution of the plant state \bar{x} as a hybrid evolution of model (9), namely

$$\bar{x}(t) = x(t, J(t)), \quad \forall t \geq 0, \quad (10)$$

where similar to [18, §8.2] for any hybrid solution x with domain $\text{dom } x$ we denote $J(t) = \min_{(t,j) \in \text{dom } x} j$.

3.2 Proposed continuous-discrete observer structure

Starting from model (9), we propose a continuous-discrete observer structure implicitly accounting for the restrictions in Assumption 2 on the available output because the flow dynamics (when the output is not available) is in open loop:

$$\dot{\hat{x}} = A\hat{x} + Bu, \quad (\tau, \sigma) \in C, \quad (11a)$$

while the jump dynamics establishes the state update when the measurement output is available. In the *jitter-tolerant* case of Definition 1, this corresponds to

$$\hat{x}^+ = \hat{x} + K_\sigma(\tau)(y_\sigma - C_\sigma \hat{x}), \quad (\tau, \sigma) \in \mathcal{D}. \quad (11b)$$

The only design parameter of our observer is matrix function $K_\sigma : [T_{m\sigma}, T_{M\sigma}] \rightarrow \mathbb{R}^{n \times m_\sigma}$ corresponding to the time-varying gain of the *discrete* output injection term. This injection depends, notably, both on the accessed output and on the elapsed time τ since the last measurement.

The jump equation (11b) becomes simpler in the *jitter free* case of Definition 1, and corresponds to

$$\hat{x}^+ = \hat{x} + \bar{K}_\sigma(y_\sigma - C_\sigma \hat{x}), \quad (\tau, \sigma) \in \mathcal{D}, \quad (11c)$$

only parameterized by the *discrete* output injection (constant) gains \bar{K}_σ , $\sigma \in \mathcal{S}_N$. Indeed, the time-varying gains $K_\sigma(\cdot)$ are only evaluated for $\tau = T_\sigma$, where

$$T_\sigma := T_{m\sigma} = T_{M\sigma}, \quad \forall \sigma \in \mathcal{S}_N. \quad (12)$$

and the output injection terms do not depend on τ .

Remark 1 *In several relevant applications (e.g., with IMU-based systems equipped with GPS sensors) the sampled measurements are combined with additional continuous-time measurements. In particular, plant (1) may be replaced by*

$$\begin{cases} \dot{x} = A_0 x + Bu + d, \\ y_c = C_c x + D_c u. \end{cases} \quad (13)$$

We may easily extend our theory to those cases by pre-designing a Luenberger gain L_c exploiting measurements y_c in continuous time to ensure some desirable properties of matrix $A_0 - L_c C_c$ (which does not need to be Hurwitz but may exhibit desirable behaviors in the observable subspaces from output y_c). Then we may replace the flow map (11a) of our continuous-discrete observer by

$$\begin{cases} \dot{\hat{x}} = A_0 \hat{x} + L_c(y_c - \hat{y}_c) + Bu, \\ \hat{y}_c = C_c \hat{x} + D_c u. \end{cases} \quad (14)$$

With this flow dynamics, the structure of the error dynamics reported in the rest of the paper remains unchanged with matrix A replaced by $A_0 - L_c C_c$ providing potentially improved continuous-time behavior as compared to the open-loop solution. The co-design of L_c and the gains $K_\sigma(\cdot)$ is beyond the scope of this paper.

3.3 Hybrid solutions and continuous-time estimate $\hat{\hat{x}}$

The presence of a lower bound $T_{m\sigma}$ between consecutive measurements ensures that the continuous-discrete observer (11) provides solutions whose domain is unbounded in the ordinary time direction t from which we may extract a continuous time estimate $t \mapsto \hat{\hat{x}}(t)$ of state x . This fact is formalized in the next proposition, whose proof is a straightforward application of [18, Prop. 6.10], because interconnection (9), (11) satisfies the Hybrid Basic Conditions [18, Ass. 6.5].

Proposition 2 *Both in the jitter-free and in the jitter-tolerant cases, all (maximal) solutions to the interconnection between (9) and (11) are complete and have an unbounded domain in the ordinary time direction t (and the jump direction j).*

Based on Proposition 2, similar to (10), we may construct a continuous-time estimate of state x by projecting the solution of the hybrid interconnection (9), (11) in the ordinary time direction t as follows

$$\hat{\hat{x}}(t) := \hat{x}(t, J(t)), \quad \forall t \geq 0. \quad (15)$$

In particular, Proposition 2 ensures t -completeness of solutions so that Zeno behavior is ruled out and we can evaluate (15) for any arbitrarily large value of t .

For proving the exponential bound (5) in Goal 1 it is sufficient to combine (10) with (15) and to prove the following hybrid t -exponential bound

$$|x(t, j) - \hat{x}(t, j)|^2 \leq M e^{-\lambda t} |x(0, 0) - \hat{x}(0, 0)|^2 + \gamma(\|d\|_{t,\infty}^2 + \|w\|_{j,\infty}^2). \quad (16)$$

This is proven in the next sections.

4 Jitter-free necessary and sufficient conditions

In this section we focus on the *jitter-free* case of Definition 1 and characterize the properties of the interconnection of plant (9) and observer (11a), (11c) introduced in the previous section. In particular, we address the analysis and design contexts highlighted after Goal 1 and provide computationally attractive necessary and sufficient analysis conditions (in terms of LMIs) and design conditions (again in terms of LMIs) for gains $\bar{K}_1, \dots, \bar{K}_N$ ensuring Goal 1.

To characterize the interconnection (9), (11a), (11c) consider the estimation error $\tilde{x} := x - \hat{x}$, whose hybrid dynamics are computed as the following autonomous system

$$\begin{cases} \dot{\tilde{x}} = A\tilde{x} + d, \quad \dot{\tau} = 1, \quad \dot{\sigma} = 0, & (\tau, \sigma) \in C, \\ \tilde{x}^+ = (I - \bar{K}_\sigma C_\sigma)\tilde{x} - \bar{K}_\sigma w, & (\tau, \sigma) \in \mathcal{D}, \\ \tau^+ = 0, \quad \sigma^+ = \Gamma(\sigma), & \end{cases} \quad (17)$$

with Γ as in (2). Based on (17) we address in two subsections the above stated analysis and design problems.

4.1 Jitter-free analysis conditions

The following theorem provides a convex (LMI-based) condition for checking whether observer (11a), (11c) with continuous-time output (15) accomplishes Goal 1. The result is based on the use of (non-necessarily common) Lyapunov-like matrices P_1, \dots, P_N . Its proof is postponed to the end of Section 5.1, to avoid breaking the flow of the exposition.

Theorem 1 Assume that there exist N matrices $P_\sigma = P_\sigma^\top > 0$, $\forall \sigma \in \mathcal{S}_N$ such that

$$\begin{bmatrix} e^{(-A^\top T_\sigma)} P_\sigma e^{(-AT_\sigma)} & \star \\ P_{\Gamma(\sigma)}(I - \bar{K}_\sigma C_\sigma) & P_{\Gamma(\sigma)} \end{bmatrix} > 0, \quad \forall \sigma \in \mathcal{S}_N. \quad (18)$$

Then observer (11a), (11c) with continuous-time output (15) accomplishes Goal 1.

The jitter-free case can be addressed in a purely discrete-time framework, e.g., using a Poincaré-type map sampling the solutions after each jump induced by the last sensor N , and then bounding the continuous-discrete intersample behavior. Due to the Round-Robin mechanism encoded in hybrid dynamics (17), this Poincaré-type map is governed by the following discrete-time state transition matrix

$$J_1 := (I - \bar{K}_N C_N) e^{AT_N} \dots (I - \bar{K}_1 C_1) e^{AT_1}, \quad (19)$$

which stems from the alternating flowing and jumping governed by C and \mathcal{D} . Since J_1 rules the sampled value of the error \tilde{x} , it is necessary for convergence to zero of $\tilde{x} = x - \hat{x}$ (and therefore also for its exponential convergence in (5) and in Goal 1) that J_1 be Schur. Then, from standard discrete-time systems theory [21, Thm 8.4] it is necessary for Goal 1 that $\exists P = P^\top > 0$ satisfying

$$P - J_1^\top P J_1 > 0. \quad (20)$$

This observation is the baseline for proving that the necessity of (18) (in addition to the sufficiency stated in Theorem 1). In particular, conditions (18) are not restrictive, which is somewhat surprising because we require all the matrices P_1, \dots, P_N to be positive definite. This necessity statement is formalized next.

Proposition 3 In the jitter-free case of (12), condition (18) is feasible if and only if observer (11a), (11c) with continuous-time output (15) accomplishes Goal 1.

Proof The sufficiency has been already proved in Theorem 1. For the necessity, it has been noted above that Goal 1 implies the existence of $P = P^\top > 0$ satisfying (20). To complete the proof, we show below that the existence of such a P implies that there exist matrices P_1, \dots, P_N satisfying

$$P_\sigma - e^{A^\top T_\sigma} (I - \bar{K}_\sigma C_\sigma)^\top P_{\Gamma(\sigma)} (I - \bar{K}_\sigma C_\sigma) e^{AT_\sigma} > 0, \quad (21)$$

which are equivalent to (18) after a Schur complement.

To this end, generalizing the definition of J_1 in (19), for each $\sigma \in \mathcal{S}_N$, define matrices

$$J_\sigma := (I - \bar{K}_N C_N) e^{AT_N} \dots (I - \bar{K}_\sigma C_\sigma) e^{AT_\sigma},$$

and note that (20) can be written as

$$P_1 - e^{A^\top T_1} (I - \bar{K}_1 C_1)^\top J_2^\top P_1 J_2 (I - \bar{K}_1 C_1) e^{AT_1} > 0 \quad (22)$$

with the selection $P_1 = P > 0$. It is then natural to select $P_2 := J_2^\top P_1 J_2 + \epsilon_2 I > 0$, with $\epsilon_2 > 0$, where positive definiteness follows from $P_1 > 0$. This selection implies (for any $\epsilon_2 > 0$) $P_2 - J_2^\top P_1 J_2 \geq \epsilon_2 I > 0$, which parallels (20). Moreover, replacing $J_2^\top P_1 J_2 = P_2 - \epsilon_2 I$ in (22), we exploit the strict inequality to prove (21) with $\sigma = 1$, for a small enough ϵ_2 . Iterating, we follow similar steps for the construction of $P_\sigma := J_\sigma^\top P_{\sigma-1} J_\sigma + \epsilon_\sigma I > 0$, $\sigma = 3, \dots, N$, and the proof is completed. \square

4.2 Jitter-free design

We propose below a convex LMI-based construction for gains \bar{K}_σ ensuring Goal 1. The ensuing conditions cannot be derived from the alternative sampled conditions (20) due to the nonlinearity w.r.t. the gains \bar{K}_σ appearing in J_1 . A sampled convex condition could be formulated by exploiting the large output matrix in (8), but such an approach is computationally less desirable, due to the large size of the ensuing LMIs, and due to the unsuitability of that approach for the jitter-tolerant case. The proof of the next theorem is given at the end of Section 5.2.

Theorem 2 Denote by C_σ^\perp a basis of the orthogonal complement of C_σ^\top for each $\sigma \in \mathcal{S}_N$. If there exists $P_\sigma = P_\sigma^\top > 0$, $\sigma = \{1, \dots, N\}$, satisfying

$$\Xi_{P_\sigma} := \begin{bmatrix} (C_\sigma^\perp)^\top e^{(-A^\top T_\sigma)} P_\sigma e^{(-AT_\sigma)} C_\sigma^\perp & \star \\ P_{\Gamma(\sigma)} C_\sigma^\perp & P_{\Gamma(\sigma)} \end{bmatrix} > 0, \quad \forall \sigma \in \mathcal{S}_N, \quad (23)$$

select

$$\bar{K}_\sigma := \left(C_\sigma^\top - C_\sigma^\perp \left((C_\sigma^\perp)^\top e^{(-A^\top T_\sigma)} P_\sigma e^{(-AT_\sigma)} C_\sigma^\perp \right)^{-1} \left(C_\sigma e^{(-A^\top T_\sigma)} P_\sigma e^{(-AT_\sigma)} C_\sigma^\perp \right)^\top \right) (C_\sigma C_\sigma^\top)^{-1}, \quad (24)$$

Then observer (11a), (11c) with continuous-time output (15) accomplishes Goal 1.

Remark 2 Note that the expression of LMIs (23) depends on the specific selection of the orthogonal complement C_σ^\perp of C_σ , which is not unique. It has been already proven in [34] (for the one sensor case) that feasibility of the LMI is independent of that selection. That proof extends straightforwardly to the multi-sensor case addressed here.

We prove below the necessity of the conditions of Theorem 2. To this end, we exploit Propositions 1 and 3. A consequence of necessity is that, as emphasized after Proposition 1, when some $T_{M\sigma}$, $\sigma \in \mathcal{S}_N$, grow too large, one expects inequalities (23) to become infeasible.

Proposition 4 *In the jitter-free case of (12), LMI (23) is feasible if and only if there exists an asymptotic observer achieving Goal 1.*

Proof The sufficiency has been already established in Theorem 2. For the necessity, from Proposition 1 if there exists an asymptotic observer achieving Goal 1, then pair (C, e^{AT}) is discrete-time detectable. Such a detectability property implies that there exist L and $Q > 0$ satisfying

$$Q - (e^{AT} - LC)^\top Q (e^{AT} - LC) > 0. \quad (25)$$

Denote $L = [L_1 \ \cdots \ L_N]$ and assume without loss of generality that matrices $(I - L_\sigma C_\sigma)$, $\sigma \in S_N$, are all invertible. If invertibility does not hold, since singular matrices are a set of measure zero, and by continuity of eigenvalues, it suffices to slightly perturb L without destabilizing the Schur eigenvalues of $(e^{AT} - LC)$.

We construct next a selection of matrices P and $\bar{K}_1, \dots, \bar{K}_N$ transforming (25) into (20). Then, via Proposition 3, (20) implies that there exist matrices P_σ satisfying (18). This proves necessity because (23) immediately follows from (18). More specifically, by initializing $H_N := I$, we select

$$\begin{cases} \bar{K}_\sigma = H_\sigma L_\sigma & \forall \sigma \in S_N, \\ H_{\sigma-1} := e^{-AT_\sigma} (I - \bar{K}_\sigma C_\sigma)^{-1} H_\sigma & \forall \sigma = 2, \dots, N. \end{cases} \quad (26)$$

Finally, introducing $\bar{T}_k := T_1 + T_2 + \dots + T_k = T_k + \bar{T}_{k-1}$, we have:

$$\begin{aligned} e^{A\bar{T}_\sigma} - \bar{K}_\sigma C_\sigma e^{A\bar{T}_\sigma} - H_\sigma \sum_{k=1}^{\sigma-1} L_k C_k e^{A\bar{T}_k} = \\ (I - \bar{K}_\sigma C_\sigma) e^{A\bar{T}_\sigma} \left((I - \bar{K}_{\sigma-1} C_{\sigma-1}) e^{A\bar{T}_{\sigma-1}} \right. \\ \left. - H_{\sigma-1} \sum_{k=1}^{\sigma-2} L_k C_k e^{A\bar{T}_k} \right) \end{aligned} \quad (27)$$

which, suitably iterated, transforms (25) in (20), and, as discussed above, the proof is completed by using Proposition 3, (18) and (23). \square

5 Jitter-tolerant sufficient conditions

We address in this section the *jitter-tolerant* context of Definition 1 for which we consider the interconnection between plant (9) and the jitter-tolerant observer (11a), (11b) providing the continuous-time estimate (15).

For this case, the error dynamics (17) governing $\tilde{x} := x - \hat{x}$ generalize to

$$\begin{cases} \dot{\tilde{x}} = A\tilde{x} + d, \quad \dot{\tau} = 1, \quad \dot{\sigma} = 0, & (\tau, \sigma) \in C, \\ \tilde{x}^+ = (I - K_\sigma(\tau)C_\sigma)\tilde{x} + K_\sigma(\tau)w, & (\tau, \sigma) \in \mathcal{D}, \\ \tau^+ = 0, \quad \sigma^+ = \Gamma(\sigma), & \end{cases} \quad (28)$$

with Γ as in (2). As compared to the jitter-free case, the set of solutions to (28) is richer in behavior, therefore we

only provide sufficient conditions ensuring Goal 1. These sufficient conditions reduce to the ones of Section 4 when the jitter reduces to zero (namely $T_{m\sigma}$ approaches $T_{M\sigma}$). Therefore we expect low conservativeness of our conditions when the jitter is small.

According to the discussion given after the statement of Goal 1, we first propose analysis conditions (with fixed gains $K_\sigma(\cdot)$) in Section 5.1 and then provide design conditions in Section 5.2. The conditions that we propose are still convex in the decision variables associated to the gains $\tau \mapsto K_\sigma(\tau)$, but the fact that these gains are infinite dimensional leads to infinite dimensional conditions. Section 5.3 gives an algorithm that is guaranteed to end in a finite number of steps, under a feasibility assumption, for solving those infinite dimensional conditions.

5.1 Stability analysis

We state below the jitter-tolerant generalization of the conditions of Theorem 1. In light of Proposition 3, we expect these sufficient conditions not to be too conservative (especially when the jitter $T_{M\sigma} - T_{m\sigma}$ is small).

Theorem 3 *Assume that there exist N matrices $P_\sigma = P_\sigma^\top > 0$, $\forall \sigma \in S_N$ such that, for each $\sigma \in S_N$,*

$$\begin{bmatrix} e^{(-A^\top \tau)} P_\sigma e^{(-A\tau)} & \star \\ P_{\Gamma(\sigma)} (I - K_\sigma(\tau)C_\sigma) & P_{\Gamma(\sigma)} \end{bmatrix} > 0, \quad \forall \tau \in [T_{m\sigma}, T_{M\sigma}]. \quad (29)$$

Then observer (11a), (11b) with continuous-time output (15) accomplishes Goal 1.

Proof: Consider the Lyapunov function:

$$V(\tilde{x}, \tau, \sigma) = e^{-\rho\tau} \tilde{x}^\top e^{(-A^\top \tau)} P_\sigma e^{(-A\tau)} \tilde{x}, \quad (30)$$

where $\rho > 0$ is a constant to be selected below, and let us emphasize that the flow and jump sets in (9d) satisfy $\mathcal{D} \subset C$, so we can concentrate on values $(\tau, \sigma) \in C$ in the following analysis. Also note that C is compact so that the following are positive quantities:

$$c_1 := \min_{(\tau, \sigma) \in C} e^{-\rho\tau} \lambda_m \left(e^{(-A^\top \tau)} P_\sigma e^{(-A\tau)} \right) > 0, \quad (31)$$

$$c_2 := \max_{(\tau, \sigma) \in C} \lambda_M \left(e^{(-A^\top \tau)} P_\sigma e^{(-A\tau)} \right) > 0. \quad (32)$$

The above-defined scalars clearly satisfy

$$c_1 |\tilde{x}|^2 \leq V(\tilde{x}, \tau, \sigma) \leq c_2 |\tilde{x}|^2, \quad \forall \tilde{x} \in \mathbb{R}^n, (\tau, \sigma) \in C. \quad (33)$$

Since $\dot{\sigma} = 0$, and consequently P_σ is constant during flow, the variation of V along the flow map of (28) becomes:

$$\begin{aligned} \dot{V} &:= e^{-\rho\tau} \tilde{x}^\top e^{(-A^\top \tau)} P_\sigma e^{(-A\tau)} (2A\tilde{x} + 2d - 2A\tilde{x}) \\ &\quad - \rho V(\tilde{x}, \tau, \sigma) \\ &\leq 2|\tilde{x}| e^{(-A^\top \tau)} P_\sigma e^{(-A\tau)} \|d\| - \rho V(\tilde{x}, \tau, \sigma) \\ &\leq 2c_F |\tilde{x}| \|d\| - \rho V(\tilde{x}, \tau, \sigma), \quad \forall (\tilde{x}, \tau, \sigma) \in \mathbb{R}^n \times C, \end{aligned} \quad (34)$$

where we defined $c_F := \max_{(\tau, \sigma) \in C} |e^{(-A^\top \tau)} P_\sigma e^{(-A\tau)}| > 0$.

Using Young's inequality, we have $2c_F |\tilde{x}| |d| \leq \frac{2c_F^2}{\rho c_1} |d|^2 + \frac{\rho c_1}{2} |\tilde{x}|^2$ that, substituted in (34), also using (33), gives

$$\dot{V} \leq -\frac{\rho}{2} V(\tilde{x}, \tau, \sigma) + \gamma_F |d|^2, \quad \forall (\tilde{x}, \tau, \sigma) \in \mathbb{R}^n \times C, \quad (35)$$

with $\gamma_F := \frac{2c_F^2}{\rho c_1}$.

The change of V across the jump map of (28) is given by

$$\begin{aligned} \Delta V &:= V(\tilde{x}^+, \tau^+, \sigma^+) - V(\tilde{x}, \tau, \sigma) \\ &= w^\top K_\sigma(\tau)^\top P_{\Gamma(\sigma)} (-2(I - K_\sigma(\tau)C_\sigma)\tilde{x} + K_\sigma(\tau)w) \\ &\quad - \tilde{x}^\top \underbrace{\left(e^{-A^\top \tau} P_\sigma e^{-A\tau} - (I - K_\sigma(\tau)C_\sigma)^\top P_{\Gamma(\sigma)} (I - K_\sigma(\tau)C_\sigma) \right)}_{M(\tau, \sigma) :=} \tilde{x} \\ &\quad + (1 - e^{-\rho \tau}) \tilde{x}^\top (e^{-A^\top \tau} P_\sigma e^{-A\tau}) \tilde{x} \\ &\leq -\tilde{x}^\top M(\tau, \sigma) \tilde{x} + c_J |w| (2|\tilde{x}| + |w|) + (e^{\rho T_M} - 1) V(\tilde{x}, \tau, \sigma), \end{aligned} \quad (36)$$

for all $(\tilde{x}, \tau, \sigma) \in \mathbb{R}^n \times C$, where we defined $T_M := \max_{\sigma \in \mathcal{S}_N} T_{M\sigma} > 0$ and $c_J := \max_{(\tau, \sigma) \in C} \{|K_\sigma(\tau)^\top P_{\Gamma(\sigma)} (I - K_\sigma(\tau)C_\sigma)|, |K_\sigma(\tau)^\top P_{\Gamma(\sigma)} K_\sigma(\tau)|\} > 0$.

Consider now (29), and use a Schur complement to get

$$e^{-A^\top \tau} P_\sigma e^{-A\tau} - (I - K_\sigma(\tau)C_\sigma)^\top P_{\Gamma(\sigma)} (I - K_\sigma(\tau)C_\sigma) > 0, \quad (37)$$

namely $M(\tau, \sigma) > 0$, $\forall (\tau, \sigma) \in C$. Since C is compact, we may define the scalar (independent of ρ):

$$c_3 := \frac{1}{c_2} \min_{(\tau, \sigma) \in C} \lambda_m(M(\tau, \sigma)) > 0. \quad (38)$$

Moreover, using Young's inequality, we may obtain the bound $2c_J |w| |\tilde{x}| \leq \frac{2c_J^2}{c_1 c_3} |w|^2 + \frac{c_1 c_3}{2} |\tilde{x}|^2$, and by selecting $\rho := T_M^{-1} \log(1 + \frac{c_3}{2})$ (recall that c_3 is independent of ρ) we may ensure that $(e^{\rho T_M} - 1) \leq \frac{c_3}{2}$. Both these inequalities can be substituted in (36) to obtain, also using (33),

$$\begin{aligned} V(\tilde{x}^+, \tau^+, \sigma^+) &\leq (1 - \frac{c_3}{2}) V(\tilde{x}, \tau, \sigma) + \gamma_J |w|^2 + (e^{\rho T_M} - 1) V \\ &\leq V(\tilde{x}, \tau, \sigma) + \gamma_J |w|^2, \quad \forall (\tilde{x}, \tau, \sigma) \in \mathbb{R}^n \times \mathcal{D}, \end{aligned} \quad (39)$$

with $\gamma_J := (c_J + \frac{2c_J^2}{c_1 c_3}) > 0$.

Consider now any solution $(t, j) \mapsto \varphi(t, j) = (\tilde{x}(t, j), \tau(t, j), \sigma(t, j))$ of (28) and note that by assumption all solutions perform infinitely many jumps (they jump at least every $T_M = \max_{\sigma \in \mathcal{S}_N} T_{M\sigma}$ ordinary time) and infinitely long flow (they flow for at least $T_m = \min_{\sigma \in \mathcal{S}_N} T_{m\sigma}$ ordinary time t after each jump). As a consequence we may use (35) together with standard comparison theory to conclude,

for all $(t, j) \in \text{dom } \varphi$,

$$V(\varphi(t, j)) \leq e^{-\frac{\rho}{2}(t-t_j)} V(\varphi(t_j, j)) + \gamma_F T_M \|d\|_{t, \infty}^2, \quad (40)$$

$$V(\varphi(t_{j+1}, j)) \leq e^{-\frac{\rho}{2} T_m} V(\varphi(t_j, j)) + \gamma_F T_M \|d\|_{t, \infty}^2, \quad (41)$$

where we used the continuous-time signal norm $\|d\|_{t, \infty}$ in (6). Furthermore, we may use (39) and the discrete-time signal norm $\|w\|_{j, \infty}$ in (6) to get

$$V(\varphi(t_j, j)) \leq V(\varphi(t_j, j-1)) + \gamma_J \|w\|_{j, \infty}^2, \quad \forall j \geq 1. \quad (42)$$

We may finally nest the bounds in (40)–(42) to get

$$\begin{aligned} V(\varphi(t, j)) &\leq e^{-\frac{\rho}{2} t} V(\varphi(0, 0)) + \sum_{k=0}^j e^{-\frac{\rho}{2} T_m k} \gamma_F T_M \|d\|_{t, \infty}^2 \\ &\quad + \sum_{k=1}^j e^{-\frac{\rho}{2} T_m k} \gamma_J \|w\|_{j, \infty}^2 \\ &\leq e^{-\frac{\rho}{2} t} V(\varphi(0, 0)) \\ &\quad + (\gamma_F T_M \|d\|_{t, \infty}^2 + \gamma_J \|w\|_{j, \infty}^2) \sum_{k=0}^{\infty} e^{-\frac{\rho}{2} T_m k} \\ &\leq e^{-\frac{\rho}{2} t} V(\varphi(0, 0)) + c_1 \gamma \|d\|_{t, \infty}^2 + c_1 \gamma \|w\|_{j, \infty}^2, \end{aligned} \quad (43)$$

where we used $R := \sum_{k=0}^{\infty} e^{-\frac{\rho}{2} T_m k} = (1 - e^{-\frac{\rho}{2} T_m})^{-1}$ and we introduced $\gamma := \frac{R}{c_1} \max\{\gamma_F T_M, \gamma_J\}$.

Applying (33) twice to (43) one obtains representation (16) of bound (5) in Goal 1 with $M = \frac{c_2}{c_1}$ and $\lambda = \frac{\rho}{2}$. \square

Proof of Theorem 1: The statement of Theorem 3 reduces to the one of Theorem 1 in the jitter-free case (12) because (29) reduces to (18) with $\tilde{K}_\sigma = K_\sigma(T_\sigma)$ for all $\sigma \in \mathcal{S}_N$. Then, Theorem 1 is a corollary of Theorem 3. \square

5.2 Observer design

We propose below a construction for gains $K_\sigma(\cdot)$ in observer (11a), (11b). The design is based on finding the Lyapunov certificates $P_\sigma = P_\sigma^\top > 0$ of the analysis conditions of Theorem 3, therefore from Proposition 4 we expect these design conditions not to be too conservative when the jitter $T_{M\sigma} - T_{m\sigma}$ is small.

Theorem 4 Assume C_σ is full row rank and denote by C_σ^\perp a basis of the orthogonal complement of C_σ^\top . If, for all $\sigma \in \mathcal{S}_N$ there exists $P_\sigma = P_\sigma^\top > 0$ satisfying

$$\begin{aligned} \Xi_{P_\sigma}(\tau) &:= \begin{bmatrix} (C_\sigma^\perp)^\top e^{(-A^\top \tau)} P_\sigma e^{(-A\tau)} C_\sigma^\perp & \star \\ P_{\Gamma(\sigma)} C_\sigma^\perp & P_{\Gamma(\sigma)} \end{bmatrix} > 0, \\ &\forall \sigma \in \mathcal{S}_N \text{ and } \forall \tau \in [T_{m\sigma}, T_{M\sigma}], \end{aligned} \quad (44)$$

select

$$K_\sigma(\tau) := \left(C_\sigma^\top - C_\sigma^\perp \left((C_\sigma^\perp)^\top e^{(-A^\top \tau)} P_\sigma e^{(-A\tau)} C_\sigma^\perp \right)^{-1} \right. \\ \left. \left(C_\sigma e^{(-A^\top \tau)} P_\sigma e^{(-A\tau)} C_\sigma^\perp \right)^\top \right) (C_\sigma C_\sigma^\top)^{-1}. \quad (45)$$

Then observer (11a), (11b) with continuous-time output (15) accomplishes Goal 1.

Proof First we may proceed as in Part 1 of [34, Thm 2] using C_σ instead of C , $\Psi_\sigma(\tau) := e^{(-A^\top \tau)} P_{\Gamma(\sigma)} e^{(-A\tau)}$ instead of $\Psi(\tau)$ and $Y_\sigma(\tau) := -P_{\Gamma(\sigma)} K_\sigma(\tau)$ instead of $Y(\tau)$ to show that condition (44) ensures the existence of a gain $K_\sigma(\cdot)$ satisfying (29).

Secondly, given matrices P_σ satisfying condition (44), we may follow the steps of Part 2 of the proof of [34, Thm 1] to obtain that (29) holds if, paralleling [34, Eq. (25)],

$$\begin{bmatrix} M_{11}^\sigma(\tau) & \star \\ M_{21}^\sigma(\tau) & M_{22}^\sigma(\tau) \end{bmatrix} := \begin{bmatrix} C_\sigma \Psi_\sigma(\tau) C_\sigma^\top & \star \\ P_{\Gamma(\sigma)} C_\sigma^\top + P_{\Gamma(\sigma)} K_\sigma(\tau) C_\sigma C_\sigma^\top & P_{\Gamma(\sigma)} \end{bmatrix} \\ - \underbrace{\begin{bmatrix} C_\sigma \Psi_\sigma(\tau) C_\sigma^\perp \\ P_{\Gamma(\sigma)} C_\sigma^\perp \end{bmatrix}}_{\Sigma_\sigma^\top} \left[(C_\sigma^\perp)^\top \Psi_\sigma(\tau) C_\sigma^\perp \right]^{-1} \Sigma_\sigma > 0, \quad (46)$$

where $\Psi_\sigma(\tau) = e^{(-A^\top \tau)} P_{\Gamma(\sigma)} e^{(-A\tau)}$. Since $M_{11}^\sigma(\cdot)$ and $M_{22}^\sigma(\cdot)$ are independent of $K_\sigma(\cdot)$, the existence result of Part 1 implies that they are both uniformly positive definite and then (46) holds with selection (45), because (45) ensures that $M_{21}^\sigma(\cdot) \equiv 0$ in (46). The proof is completed by applying Theorem 3. \square

Proof of Theorem 2: The statement of Theorem 4 reduces to the one of Theorem 2 in the jitter-free case (12) because (44) reduces to (23). Then, Theorem 2 is a corollary of Theorem 4. \square

Remark 3 As discussed in [23, §4.3.6–4.3.7], discrete-time and linear parameter varying (LPV) approaches to deal with time-varying sampling intervals can provide an alternative approach to the one considered in this paper. Hence, inspired by [19], [20] and [36], a discrete-time LPV framework could be used to design an observer, robust to the non-constant intersample time induced by the bounds $T_{m\sigma(t_k)}$ and $T_{M\sigma(t_k)}$. The alternative hybrid techniques used here allow deriving necessary and sufficient conditions in the jitter-free case, which become only sufficient in the jitter-tolerant case. These conditions are independent of the observer gains, thanks to the use of the elimination lemma.

5.3 Design algorithm

In this section the main ingredients of the algorithm presented in [34] are generalized for solving the infinite-dimensional problem (44) in a finite number of steps. As in [34], the algorithm consists in three steps (the initialization, the synthesis, and the analysis phase) as described below.

- *Step 1. Initialization.* Constants β and γ satisfying $(A +$

$\beta I)^\top \Pi + \Pi(A + \beta I) > 0$ and $\gamma := \sqrt{\lambda_M(\Pi)/\lambda_m(\Pi)}$, for some $\Pi = \Pi^\top > 0$ are selected. This step is based on [34, Lemma 3].

- *Step 2. Synthesis.* We solve the finite dimensional optimization:

$$(P_1^*, \dots, P_N^*, p^*) = \arg \min_{P_\sigma = P_\sigma^\top, p_M} p_M, \quad \text{s.t.} \quad (47) \\ \Xi_{P_\sigma}(\tau) > 2\mu I, \quad \forall \tau \in \mathcal{T}_\sigma \text{ and } \forall \sigma \in \mathcal{S}_N, \\ I \leq P_\sigma \leq p_M I, \quad \forall \sigma \in \mathcal{S}_N$$

where τ ranges over a finite number of points collected in the discrete sets \mathcal{T}_σ (in the first step $\mathcal{T}_\sigma = \{T_{m\sigma}, T_{M\sigma}\}$).

- *Step 3. Analysis.* Given $(P_1^*, \dots, P_N^*, p^*)$ from (47), we check the following eigenvalue conditions, relaxing the constraints in (47) to half of their values:

$$\Xi_{P_\sigma^*}(\tau) > \mu I, \quad \forall \tau \in \mathcal{T}_{d\sigma} \text{ and } \forall \sigma \in \mathcal{S}_N \quad (48)$$

where $\mathcal{T}_{d\sigma} \subset [T_{m\sigma}, T_{M\sigma}]$, $\forall \sigma \in \mathcal{S}_N$, contains an ordered set of scalars $T_{m\sigma} = \tau_1^\sigma < \dots < \tau_{\nu^\sigma}^\sigma = T_{M\sigma}$ satisfying:

$$\tau_{k+1}^\sigma - \tau_k^\sigma \leq 2\delta^* := \frac{2\mu}{p^* \|A\| \gamma e^{\beta T_M}}, \quad \forall k \text{ and } \forall \sigma \in \mathcal{S}_N, \quad (49)$$

where $T_M = \max_{\sigma \in \mathcal{S}_N} T_{M\sigma}$.

Finally, if all of the N conditions (48) are satisfied, then the algorithm stops and gives (P_1^*, \dots, P_N^*) as solutions to (44). Otherwise, for each violation of (48), a value:

$$\bar{\tau}_\sigma \in \arg \min_{\tau \in \mathcal{T}_{d\sigma}} (\lambda_m(\Xi_{P_\sigma^*}(\tau))) \quad (50)$$

is added to the corresponding set \mathcal{T}_σ , and the algorithm restarts from the synthesis phase (i.e. Step 2).

Regarding the convergence of this algorithm, the following theorem can be stated.

Theorem 5 If there exist solutions P_σ , $\forall \sigma \in \mathcal{S}_N$, to problem (44), then the proposed algorithm terminates successfully providing outputs $(P_1^*, \dots, P_N^*, p^*)$, after a finite number of iterations.

Proof The proof follows the same technique as that of [34, Thm 3] with the caveat of considering the worst case among all $\sigma \in \mathcal{S}_N$ of the quantities defined therein. Similar to [34, Thm 3], the number of iterations depends on the condition numbers of P_σ , $\forall \sigma \in \mathcal{S}_N$. \square

6 Numerical example

Consider the quarter-car active automotive suspension system shown in Fig. 2. The state-space model of this system can be written as [33]:

$$\dot{x} = Ax + B_u F_a + B_d \dot{z}_r + d, \quad (51)$$

where F_a is the active force of an actuator, d is the process disturbance, \dot{z}_r is an input that models how the road profile enters into the system, the state vector $x = [x_1 \ x_2 \ x_3 \ x_4]^\top$,

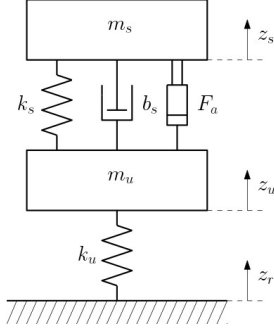


Fig. 2. Quarter-car active automotive suspension system.

comprises the suspension deflection $x_1 = z_s - z_u$, the absolute velocity $x_2 = \dot{z}_s$ of the sprung mass m_s , the tire deflection $x_3 = z_u - z_r$, and the absolute velocity $x_4 = \dot{z}_u$ of the unsprung mass m_u . A , B_u and B_d are given by:

$$A = \begin{bmatrix} 0 & 1 & 0 & -1 \\ -\frac{k_s}{m_s} & -\frac{b_s}{m_s} & 0 & \frac{b_s}{m_s} \\ 0 & 0 & 0 & 1 \\ \frac{k_s}{m_u} & \frac{b_s}{m_u} & -\frac{k_t}{m_u} & -\frac{b_s+b_t}{m_u} \end{bmatrix}, \quad B_u = \begin{bmatrix} 0 \\ \frac{1}{m_s} \\ 0 \\ -\frac{1}{m_u} \end{bmatrix}, \quad B_d = \begin{bmatrix} 0 \\ 0 \\ -1 \\ \frac{b_t}{m_u} \end{bmatrix}.$$

The following parameters are considered in the model: $k_s = 1.6 \cdot 10^4$, $b_s = 10^3$, $m_s = 250$, $m_u = 45$, $k_t = 400$, $b_t = 0$. The process disturbance d is selected as $d := [d_1, d_2, d_3, d_4]^T$, where d_1, \dots, d_4 are zero mean uniformly distributed random noises such that: $\|d_1\|_{t,\infty} = 0.004$, $\|d_2\|_{t,\infty} = 0.1$, $\|d_3\|_{t,\infty} = 0.04$, $\|d_4\|_{t,\infty} = 0.1$.

In order to apply the proposed algorithm to estimate the state vector of system (51) we assume to measure sequentially the components x_1 and x_3 . This means that $N = 2$ and $\mathcal{S}_N = \mathcal{S}_2 = \{1, 2\}$, and the output matrices are $C_1 = [1 \ 0 \ 0 \ 0]$ and $C_2 = [0 \ 0 \ 1 \ 0]$. Moreover, we assume that both measurements are corrupted by a zero mean uniformly distributed random noise w , in particular the measurement of x_1 is corrupted by a random noise w_1 with $\|w_1\|_{t,\infty} = 0.002$, while the measurement of x_3 is corrupted by a random noise w_2 with $\|w_2\|_{t,\infty} = 0.02$. We also select the interval $[T_{m\sigma}, T_{M\sigma}]$ equal to $[0.02, 0.07]$ for $\sigma = 1$ and equal to $[0.04, 0.09]$ for $\sigma = 2$. Finally, the orthogonal

complements of C_1 and C_2 are selected as $C_1^\perp = \begin{bmatrix} 0 & 0 & 0 \\ 1 & 0 & 0 \\ 0 & 1 & 0 \\ 0 & 0 & 1 \end{bmatrix}$,

$C_2^\perp = \begin{bmatrix} 0 & -1 & 0 \\ 1 & 0 & 0 \\ 0 & 0 & 0 \\ 0 & 0 & 1 \end{bmatrix}$. In order to find matrices P_σ , $\sigma \in \{1, 2\}$,

satisfying (44) for all $(\tau, \sigma) \in \bigcup_{\sigma \in \mathcal{S}_2} ([T_{m\sigma}, T_{M\sigma}] \times \{\sigma\})$, we apply the algorithm described in Section 5.3. In this case the algorithm finds a solution after three steps. Indeed, as shown in Fig. 3 (left), the validation phase initially fails because not all of the sampled minimum eigenvalues of matrix $\Xi_{P_1}(\tau)$ are positive. For this reason the value $\bar{\tau} = 0.0534$, associated to the minimum over τ of $\lambda_m(\Xi_{P_1}(\tau))$ is included in the set \mathcal{T} . Then the algorithm restarts from the synthesis phase with one extra constraint. After this second iteration the algorithm finds a second solution, which again fails to satisfy the validation phase, and the value $\bar{\tau} = 0.0434$ is included in the set \mathcal{T} (see Fig. 3 (middle)). Finally, at the

third iteration, the algorithm finds a solution satisfying the validation phase, as shown in Fig. 3 (right). The matrices P_σ , $\sigma \in \{1, 2\}$ solving (44), can be normalized for better numerical conditioning (indeed (44) is homogeneous), thus obtaining:

$$P_1 = \begin{bmatrix} 11.5 & -2.3 & -1.6 & -1.1 \\ -2.3 & 5.5 & -2.1 & 4.5 \\ -1.6 & -2.1 & 11.5 & -1.3 \\ -1.1 & 4.5 & -1.3 & 4.2 \end{bmatrix}, \quad P_2 = \begin{bmatrix} 12.5 & -0.8 & -0.9 & -1.0 \\ -0.8 & 0.8 & 0.9 & 0.9 \\ -0.9 & 0.9 & 0.9 & 0.1 \\ -1.0 & 0.9 & 0.1 & 1.1 \end{bmatrix}. \quad (52)$$

The dynamics (51) has been implemented together with the continuous-discrete observer (11) in the MATLAB®-Simulink environment. The gains $K_\sigma(\tau)$ are computed on-line according to (45) by using matrices P_σ , $\sigma \in \{1, 2\}$, in (52). Moreover, to simulate random measurements instants, we implemented the following modified stochastic hybrid dynamical version of the error dynamics, corresponding to (28) with a random selection of the inter-measurement intervals:

$$\begin{aligned} \dot{\tilde{x}} &= A\tilde{x} + d, \quad \dot{\tau} = 1, \quad \dot{\sigma} = 0, \quad \dot{\tau}_r = -1, \quad \tau_r > 0, \\ \begin{cases} \tilde{x}^+ = (I - K_\sigma(\tau)C_\sigma)\tilde{x} + K_\sigma(\tau)w, \\ \tau^+ = 0, \quad \sigma^+ = \Gamma(\sigma), \\ \tau_r^+ = T_{m\sigma} + (T_{M\sigma} - T_{m\sigma})v^+, \end{cases} & \tau_r = 0, \end{aligned} \quad (53)$$

where v^+ is a random variable uniformly distributed in the set $[0, 1]$. The results of the numerical simulation are shown in Figs. 4 and 5. In particular, from the bottom trace in Fig. 4 we note that the Lyapunov function V in (30) decreases, due to the persistent jumps, as expected from the theoretical results of Theorem 3. Also the output estimation error converges close to zero as shown in the top traces of Fig. 4. Due to the persistence of the process disturbance d and measurement noise w , the error does not converge to zero, but remains bounded, according to the ISS bound (5) given in Goal 1. Finally, from the evolution of τ in Fig. 5, we see that the jumps occur randomly within the prescribed intervals, according to dynamics (53).

7 Conclusions

A time-varying sampled-data observer has been proposed for linear systems whose outputs are sequentially sampled via non-uniform sampling intervals repeating a prescribed Round-Robin sequence. When the sampling intervals are constant (jitter-free case) necessary and sufficient conditions have been provided for the design of an asymptotic continuous-discrete observer whose estimation error is ISS from process disturbances and measurement noise. With jitter-tolerant sampling intervals, sufficient conditions for ISS asymptotic estimation have been given, and a constructive design technique has been proposed. A numerical example based on a practical application has been discussed, showing the effectiveness of the proposed approach.

References

- [1] T. Ahmed-Ali and F. Lamnabhi-Lagarrigue. High gain observer design for some networked control systems. *IEEE Transactions on Automatic Control*, 57(4):995–1000, 2012.

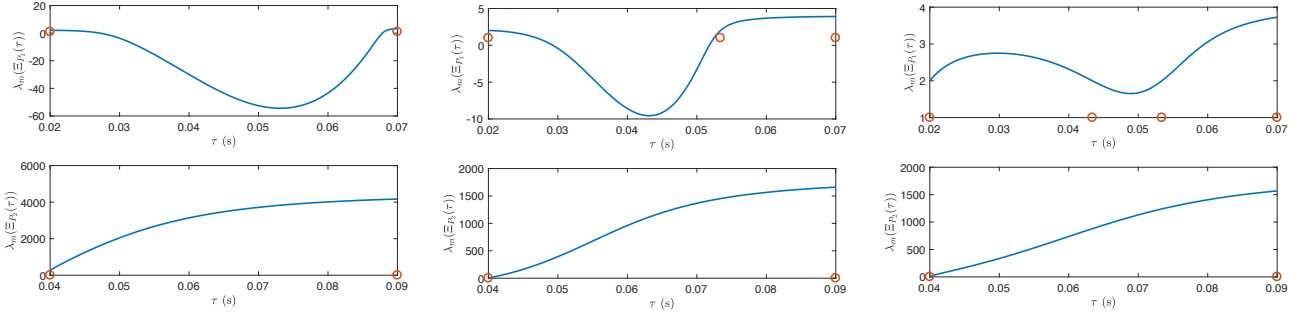


Fig. 3. Minimum eigenvalues of matrices $\Xi P_1(\tau)$ for $\tau \in [0.02, 0.07]$ (top plots), and $\Xi P_2(\tau)$ for $\tau \in [0.04, 0.09]$ (bottom plots) after: the first iteration (left), the second iteration (middle) and the third iteration (right).

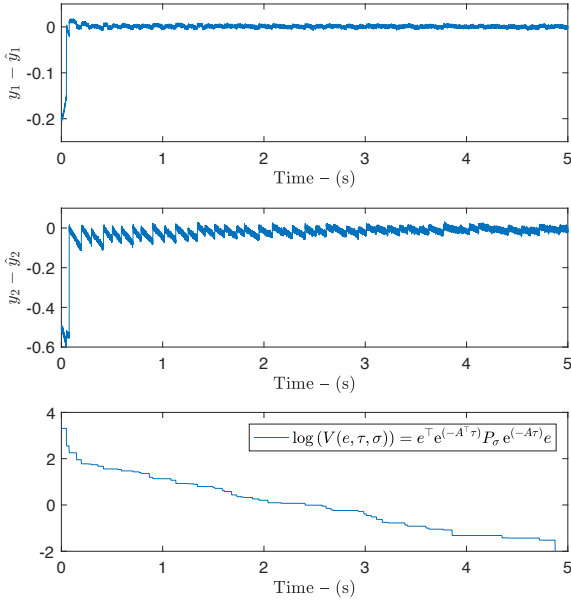


Fig. 4. Top two traces: evolution of the output errors. Bottom trace: evolution of $\log(V)$, with V defined in (30).

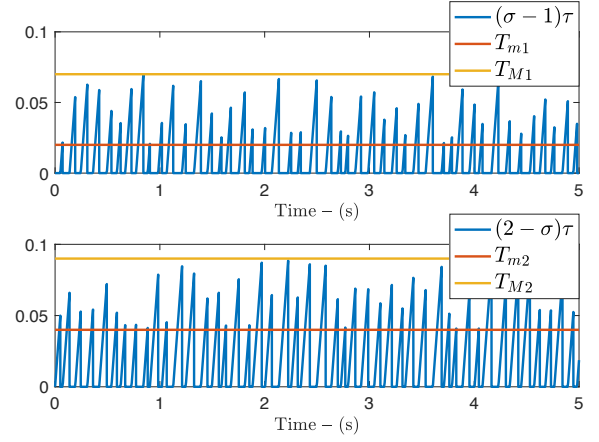


Fig. 5. Evolution of the timer and related upper and lower bounds. The upper plot, showing $(\sigma - 1)\tau$ is informative when $\sigma = 2$ and zero when $\sigma = 1$. Viceversa, the lower plot, showing $(2 - \sigma)\tau$, is informative when $\sigma = 1$ and zero when $\sigma = 2$.

- [2] F. Alonge, F. D'Ippolito, G. Garraffa, and A. Sferlazza. Hybrid observer for indoor localization with random time-of-arrival measurements. In *IEEE-RTSI*, pages 1–6. IEEE, 2018.
- [3] V. Andrieu and M. Nadri. Observer design for lipschitz systems with discrete-time measurements. In *IEEE-CDC*, pages 6522–6527. IEEE, 2010.
- [4] V. Andrieu, M. Nadri, U. Serres, and J.-C. Vivalda. Continuous discrete observer with updated sampling period. *IFAC Proceedings Volumes*, 46(23):439–444, 2013.
- [5] M. Arcak and D. Nešić. A framework for nonlinear sampled-data observer design via approximate discrete-time models and emulation. *Automatica*, 40(11):1931–1938, 2004.
- [6] A. Barrau and S. Bonnabel. Invariant Kalman filtering. *Review of Control, Robotics, and Autonomous Systems*, 1:237–257, 2018.
- [7] C. Cai and A. Teel. Characterizations of input-to-state stability for hybrid systems. *Systems & Control Letters*, 58(1):47–53, 2009.
- [8] C. Cai, A. Teel, and R. Goebel. Smooth Lyapunov functions for hybrid systems Part II: (pre) asymptotically stable compact sets. *IEEE Transactions on Automatic Control*, 53(3):734–748, 2008.
- [9] T. Chen and B. A. Francis. *Optimal sampled-data control systems*. Springer Science & Business Media, 2012.

- [10] M. B. Cloosterman, L. Hetel, N. Van de Wouw, W. Heemels, J. Daafouz, and H. Nijmeijer. Controller synthesis for networked control systems. *Automatica*, 46(10):1584–1594, 2010.
- [11] D. Dačić and D. Nešić. Observer design for wired linear networked control systems using matrix inequalities. *Automatica*, 44(11):2840–2848, 2008.
- [12] T. N. Dinh, V. Andrieu, M. Nadri, and U. Serres. Continuous-discrete time observer design for lipschitz systems with sampled measurements. *IEEE Transactions on Automatic Control*, 60(3):787–792, 2015.
- [13] M. Farza, M. M'Saad, M. L. Fall, E. Pigeon, O. Gehan, and K. Busawon. Continuous-discrete time observers for a class of MIMO nonlinear systems. *IEEE Transactions on Automatic Control*, 59(4):1060–1065, 2014.
- [14] A. Feddaoui, N. Boizot, E. Busvelle, and V. Hugel. A Kalman filter for linear continuous-discrete systems with asynchronous measurements. In *IEEE-CDC*, pages 2813–2818. IEEE, 2017.
- [15] A. Feddaoui, N. Boizot, E. Busvelle, and V. Hugel. High-gain extended Kalman filter for continuous-discrete systems with asynchronous measurements. *Int. J. of Control*, pages 1–14, 2018.
- [16] F. Ferrante, F. Gouaisbaut, R. G. Sanfelice, and S. Tarbouriech. State estimation of linear systems in the presence of sporadic measurements. *Automatica*, 73:101–109, 2016.
- [17] F. Ferrante, F. Gouaisbaut, R. G. Sanfelice, and S. Tarbouriech. \mathcal{L}_2 state estimation with guaranteed convergence speed in the presence

- of sporadic measurements. *IEEE Transactions on Automatic Control*, 64(8):3362–3369, 2019.
- [18] R. Goebel, R. G. Sanfelice, and A. R. Teel. *Hybrid Dynamical Systems: modeling, stability, and robustness*. Princeton University Press, 2012.
 - [19] M. Halimi, G. Millerioux, and J. Daafouz. Polytopic observers for LPV discrete-time systems. In *Robust Control and Linear Parameter Varying Approaches*, pages 97–124. Springer, 2013.
 - [20] W. M. H. Heemels, J. Daafouz, and G. Millerioux. Observer-based control of discrete-time LPV systems with uncertain parameters. *IEEE transactions on automatic control*, 55(9):2130–2135, 2010.
 - [21] J. P. Hespanha. *Linear systems theory*. Princeton Univ press, 2018.
 - [22] J. P. Hespanha, P. Naghshtabrizi, and Y. Xu. A survey of recent results in networked control systems. *Proceedings of the IEEE*, 95(1):138–162, 2007.
 - [23] L. Hetel, C. Fiter, H. Omran, A. Seuret, E. Fridman, J. Richard, and S. Niculescu. Recent developments on the stability of systems with aperiodic sampling: An overview. *Automatica*, 76:309–335, 2017.
 - [24] S. Kluge, K. Reif, and M. Brokate. Stochastic stability of the extended Kalman filter with intermittent observations. *IEEE Transactions on Automatic Control*, 55(2):514–518, 2010.
 - [25] Y. Li, S. Phillips, and R. G. Sanfelice. Robust distributed estimation for linear systems under intermittent information. *IEEE Transactions on Automatic Control*, 63(4):973–988, 2018.
 - [26] M. Nadri, H. Hammouri, and C. Astorga. Observer design for continuous-discrete time state affine systems up to output injection. *European journal of control*, 10(3):252–263, 2004.
 - [27] M. Nadri, H. Hammouri, and R. M. Grajales. Observer design for uniformly observable systems with sampled measurements. *IEEE Transactions on Automatic Control*, 58(3):757–762, 2013.
 - [28] D. Nešić, A. R. Teel, and E. D. Sontag. Formulas relating \mathcal{KL} stability estimates of discrete-time and sampled-data nonlinear systems. *Systems & Control Letters*, 38(1):49–60, 1999.
 - [29] S. Phillips, R. S. Erwin, and R. G. Sanfelice. Robust exponential stability of an intermittent transmission state estimation protocol. In *American Control Conference*, pages 622–627. IEEE, 2018.
 - [30] K. Plarre and F. Bullo. On Kalman filtering for detectable systems with intermittent observations. *IEEE Transactions on Automatic Control*, 54(2):386–390, 2009.
 - [31] R. Postoyan and D. Nesic. A framework for the observer design for networked control systems. *IEEE Transactions on Automatic Control*, 57(5):1309–1314, 2011.
 - [32] T. Raff, M. Kögel, and F. Allgöwer. Observer with sample-and-hold updating for lipschitz nonlinear systems with nonuniformly sampled measurements. In *IEEE-ACC*, pages 5254–5257. IEEE, 2008.
 - [33] R. Rajamani. *Vehicle dynamics and control*. Springer Science, 2011.
 - [34] A. Sferlazza, S. Tarbouriech, and L. Zaccarian. Time-varying sampled-data observer with asynchronous measurements. *IEEE Transactions on Automatic Control*, 64(2):869–876, 2019.
 - [35] B. Sinopoli, L. Schenato, M. Franceschetti, K. Poolla, M. Jordan, and S. S. Sastry. Kalman filtering with intermittent observations. *IEEE Transactions on Automatic Control*, 49(9):1453–1464, 2004.
 - [36] R. Tóth. *Modeling and identification of linear parameter-varying systems*, volume 403. Springer, 2010.
 - [37] Y. Xu and J. P. Hespanha. Estimation under uncontrolled and controlled communications in networked control systems. In *IEEE-CDC*, pages 842–847. IEEE, 2005.
 - [38] Z. Zhou, Y. Li, J. Zhang, and C. Rizos. Integrated navigation system for a low-cost quadrotor aerial vehicle in the presence of rotor influences. *Journal of Surveying Engineering*, 143(1):1–13, 2016.